Supporting Information

Effects of the Chemical Structure, Surface, and Micropore Properties of Activated and Oxidized Black Carbon on the Sorption and Desorption of Phenanthrene

Shujie Hu[a,b], Dainan Zhang[a], Yu Yang[a], Yong Ran[a,*], Jingdong Mao[c], Wenying Chu[c], Xiaoyan Cao[d]

[a] *State Key Laboratory of Organic Geochemistry, Guangzhou Institute of Geochemistry, Chinese Academy of Sciences, Guangzhou, 510640, China*

[b] *University of Chinese Academy of Science, Beijing 100049, China*

[c] *Department of Chemistry and Biochemistry, Old Dominion University, Norfolk, Virginia 23529, United States*

[d] *Department of Chemistry, Brandeis University,Waltham, MA 02453, USA*

[*] Corresponding authors: 86-20-85290263 (phone), 86-20-85290706 (fax), e-mail: yran@gig.ac.cn (Yong Ran)

Activated methods, Batch sorption and desorption experiments, Sorption models, 8 Tables, 14 Figures, 32 pages in total

Contents:

1. Activated methods
2. Batch sorption and desorption experiments
3. Sorption models
4. Table S1. Elemental compositions and extractable organic matter for Z-BCs before and after the solvent extraction.
5. Table S2. Elemental compositions and surface properties of the $ZnCl_2$ activated and oxidized BCs.
6. Table S3. Elemental compositions and surface properties of the KOH activated and oxidized BCs.
7. Table S4. Structural parameters derived from MultiCP/MAS ^{13}C NMR.
8. Table S5. Micropore volumes and mesopore volumes for Z-BCs before and after the solvent extraction
9. Table S6. Micropore volumes and mesopore volumes on the activated and oxidized BCs.
10. Table S7. Sorption parameters of phenanthrene of BCs obtained by the *DR* model.
11. Table S8. Freundlich parameters for the sorption and desorption, and hysteresis index of benzene on inactivated BCs*.
12. Figure S1. Carbon dioxide adsorption isotherms of BCs.
13. Figure S2. Micropore size distributions of BCs.
14. Figure S3. N_2 adsorption and desorption isotherms of BCs
15. Figure S4. Sorption isotherms of phenanthrene on $ZnCl_2$- or KOH- activated and

oxidized BCs.

16. Figure S5. Sorption and desorption isotherms of phenanthrene on extracted $ZnCl_2$-activated BCs.

17. Figure S6. The relationships among the *n* values of phenanthrene with the values of H/C and CO_2-V_o on BCs.

18. Figure S7. The relationships between the sorption capacity log K_{OC} of phenanthrene and the polarity factor (N+O)/C on BCs. In the graph, the black dots and lines represent C_e=0.01S_w, the red dots and lines C_e=0.1S_w, and the blue dots and lines C_e=S_w.

19. Figure S8. The relationships among the log K_{OC} (C_e=0.01S_w) values of phenanthrene with CEC values and surface amphoteric properties on $ZnCl_2$ or KOH activated and oxidized BCs.

20. Figure S9. The relationships between the HI values and the V_o values on BCs. Graph (a) was the desorption of phenanthrene on E-Z-BCs and graph (b) was the desorption of benzene on inactivated kerogen BCs.

21. Figure S10. The relationships between the sorption capacity log K_{OC} of phenanthrene and the micropore volumes (CO_2-V_o) on BCs. In the graph, the black dots and lines represent C_e=0.01S_w, the red dots and lines C_e=0.1S_w, and the blue dots and lines C_e=S_w.

22. Figure S11. The relationships between logK_{OC} (C_e=0.01S_w) values of phenanthrene and polar carbon on the $ZnCl_2$ or KOH activated and oxidized BCs. (In the graph, black lines are E-Z-BCs, ZHP-BCs, and ZSH-BCs, red lines are

PHP-BCs and PSH-BCs, and blue lines are inactivated kerogen-derived samples. The outlier of PSH500 was shown in the red blank circle and not included in the corresponding correlation equation.)

23. Figure S12. The relationships of the log K_{OC} and n of phenanthrene with F_{aro}%, F_{naro}%, and F_{Haro}% on the BCs. In the graph, the gray lines represent the ZHP-BCs and ZSH-BCs, the pink lines represent the PHP-BCs and PSH-BCs, and the blue lines represent the inactivated kerogen-derived BCs. The black dots represent OS and are included in the correlation equation.

24. Figure S13. Sorption isotherms of phenanthrene on BCs described by the *DR* model.

25. Figure S14. The relationships between the adsorption volumes Q_o' of phenanthrene and the DFT-$V_{(0.37\text{-}1.1nm)}$/DFT-V_o% on BCs.

1. Activated methods

Briefly, the $ZnCl_2$-activated black carbon was produced by impregnation with $ZnCl_2$, followed by slow pyrolysis under an oxygen-limited condition as previously reported.[1] Firstly, the kerogen was impregnated in $ZnCl_2$ solution for 12 h at $ZnCl_2$/kerogen mass ratio of 1.[2-5] Then the mixture was dried at 105 °C before a thermal treatment. 10 g of the powered sample was sealed in a steel ampoule. Before pyrolysis, the headspace was purged with N_2 for at least 1 min prior to sealing the steel ampoule. Six ampoules were heated in a temperature programing muffle furnace ranging from 25 °C to 200 °C at 20 °C/min and at 2 °C/min reach in 500 °C . When the pyrolysis temperature reached 250 °C, 300 °C, 350 °C, 400 °C, 450 °C, and 500 °C, a steel ampoule was removed. The thermal treatment was repeated two times. After the thermal treatment, the resulting solids were washed with 0.1 M HCl to leach out the activating agent, followed by distilled water several times to remove excess acid. The residues were freeze-dried and ground. For the KOH-activated BCs, the kerogen was impregnated with aqueous solutions of KOH with a ratio of 1:1 for 2 h at 60 °C.[5-8] Then the mixture was treated like the $ZnCl_2$-activated treatment. At the end of the thermal treatment, the products were washed with 5 M HCl, followed by distilled water until the neutral condition.

2. Batch sorption and desorption experiments

In brief, ten initial concentrations of phenanthrene ranged from 10 to 1,000 μg/L, and each point was run in duplicate. The specific solids to solution ratios were

adjusted so that the amount of adsorption at equilibrium was between 30-80% of the initial concentration. The vials were sealed with a blue flame to prevent any phenanthrene vapor losses and then placed on a shaker at 125 rmp for 28 d to achieve the sorption equilibrium. Preliminary tests showed that the apparent sorption equilibrium was reached at day 14 for the shale or kerogen derived BCs. Desorption was performed by replacing the 80% of the supernatant with the phenanthrene free background solution for the sorbate–sorbent systems. The vials were sealed with a blue flame and then placed on a shaker at 125 rmp for 14 d to achieve the desorption equilibrium. After reaching sorption or desorption equilibrium, the vials were settled for 3 d to allow the suspended solids to settle. In order to prevent the adsorption of phenanthrene on the wall of the glass bottle, 2 mL of the suspension was mixed with 1 mL of methanol and added to a 4 mL glass bottle, and then the homogeneous suspension and methanol were transferred to a 1.5 mL cell flask for assay. The concentration of phenanthrene was measured by using a high-performance liquid chromatograph (HPLC) (LC-20A, Shimadzu, Japan) equipped with fluorescence detector and Inertsil ODS-SP reverse-phase column (150 mm × 4.6 mm × 5 μm). The injection volume was 10 μL with a flow rate of 1.0 mL/min, and the mobile phase consisted of 90% acetonitrile/10% water for phenanthrene. The excitation and emission wavelengths for the detector were 250 nm and 364 nm for phenanthrene, respectively.

3. Sorption and desorption models

The Freundlich isotherm is the most common model for describing the sorption and desorption of HOCs by heterogeneous adsorbents.[9, 10] The Freundlich model has the following Eq. S1:

$$\log q_e = \log K_F + n \log C_e \qquad \text{(S1)}$$

Where q_e (μg/g) and C_e (μg/L) are the equilibrium solid-phase and aqueous-phase solute concentration, respectively; K_F is the sorption affinity-related parameter ((μg/g)/ (μg/L)^n); and n is the isotherm nonlinearity index.

The Dubinin-Radushkevitch (*DR*) isotherm model[11, 12] has the following Eq. S2:

$$\log q_e' = \log(Q_0') - D(\log S_{scl}/C_e)^2 \qquad \text{(S2)}$$

where q_e' is the adsorbed solute volume per unit mass of sorbent (cm^3/kg); Q_o' is the maximum volume adsorbed (cm^3/kg); S_{scl} and C_e are the supercooled liquid-state solubility and the equilibrium concentration of the solute at temperature T (K), respectively; and D is a constant related to the energy of adsorption and the pore structure.

Table S1. Elemental compositions and extractable organic matter for Z-BCs before and after the solvent extraction.

Sample	C%	H%	N%	O%	CHNO%	H/C	O/C	(N+O)/C	Extractable organic matter mg/g	Water contact angle
Z250	71.2	6.51	2.32	17.8	97.9	1.10	0.19	0.22	66.5	128°
Z300	75.0	5.71	2.45	14.1	97.3	0.91	0.14	0.17	74.7	109°
Z350	75.9	4.85	2.51	13.8	97.0	0.77	0.14	0.16	29.7	83.8°
Z400	76.0	4.62	2.32	17.4	100	0.73	0.17	0.20	8.97	<10°
Z450	75.6	5.03	2.24	19.2	102	0.80	0.19	0.22	11.3	<10°
Z500	75.6	5.54	2.23	20.4	104	0.88	0.20	0.23	9.13	<10°
After solvent extraction										
E-Z250	66.9	7.67	1.92	22.3	98.8	1.37	0.25	0.27	--	106°
E-Z300	69.1	5.80	2.56	18.0	95.4	1.01	0.20	0.23	--	115°
E-Z350	71.6	5.48	2.22	16.7	96.1	0.92	0.18	0.20	--	82.3°
E-Z400	73.8	5.33	2.58	17.6	99.3	0.87	0.18	0.21	--	<10°
E-Z450	74.3	4.59	2.51	20.7	102	0.74	0.21	0.24	--	<10°
E-Z500	74.8	5.39	2.01	19.1	101	0.86	0.19	0.21	--	<10°

Table S2. Elemental compositions and surface properties of the $ZnCl_2$ activated and oxidized BCs.

Sample	C%	H%	N%	O%	CHNO%	H/C	O/C	(N+O)/C	Surface Acidic groups (mmol/g)				Surface Basic groups (mmol/g)	CEC (cmol/kg)	Water contact angle
									Carboxyl groups	Lactonic groups	Phenolic groups	Total Acidic groups			
OS	67.6	6.62	2.22	19.4	95.8	1.17	0.21	0.24	nd	0.18	4.61	4.79	0.23	35.7	105°
ZHP250	68.4	6.05	2.06	20.5	97.0	1.06	0.22	0.25	nd	nd	4.86	4.86	1.28	140	122°
ZHP300	71.1	5.26	2.19	18.0	96.5	0.89	0.19	0.22	nd	nd	4.51	4.51	1.56	116	97.9°
ZHP350	73.0	4.48	2.36	17.6	97.5	0.74	0.18	0.21	nd	nd	3.79	3.79	1.60	183	57.9°
ZHP400	72.4	4.16	2.09	20.3	99.0	0.69	0.21	0.23	nd	nd	3.71	3.71	1.41	185	<10°
ZHP450	70.6	4.48	1.86	24.3	101	0.76	0.26	0.28	nd	nd	3.35	3.35	1.48	222	<10°
ZHP500	69.9	4.74	1.91	28.1	105	0.81	0.30	0.32	nd	nd	3.82	3.82	1.61	208	<10°
ZSH250	62.9	5.24	1.64	18.7	88.5	1.00	0.22	0.25	nd	nd	7.24	7.24	1.40	132	112°
ZSH300	65.2	4.64	1.90	16.6	88.3	0.85	0.19	0.22	nd	nd	6.05	6.05	1.15	80.2	102°
ZSH350	66.9	3.93	1.92	17.8	90.5	0.70	0.20	0.22	nd	nd	6.05	6.05	1.19	98.4	33.0°
ZSH400	65.0	3.59	1.64	20.9	91.1	0.66	0.24	0.26	nd	nd	5.49	5.49	1.03	36.2	<10°
ZSH450	65.7	3.87	1.65	24.9	96.1	0.71	0.28	0.31	nd	nd	4.66	4.66	1.28	151	<10°
ZSH500	67.7	4.32	1.59	26.7	100.4	0.77	0.30	0.32	nd	nd	3.63	3.63	1.33	157	<10°

Table S3. Elemental compositions and surface properties of the KOH activated and oxidized BCs.

Sample	C%	H%	N%	O%	CHNO%	H/C	O/C	(N+O)/C	Surface Acidic groups (mmol/g)				Surface Basic groups (mmol/g)	CEC (cmol/kg)	Water contact angle
									Carboxyl groups	Lactonic groups	Phenolic groups	Total Acidic groups			
PHP250	66.5	6.40	1.72	21.6	96.2	1.16	0.24	0.27	nd	nd	6.90	6.90	1.18	134	125°
PHP300	68.8	6.25	1.92	19.4	96.3	1.09	0.21	0.23	nd	nd	5.78	5.78	1.33	154	124°
PHP350	73.3	6.11	2.19	14.8	96.4	1.00	0.15	0.18	nd	0.26	3.81	4.07	nd	145	122°
PHP400	75.7	4.58	2.66	13.7	96.7	0.73	0.14	0.17	nd	nd	4.50	4.50	nd	177	94.2°
PHP450	70.6	3.44	2.64	19.1	95.8	0.58	0.20	0.23	nd	nd	4.36	4.36	nd	148	<10°
PHP500	71.0	3.22	2.61	19.2	96.1	0.54	0.20	0.23	nd	nd	6.18	6.18	0.31	196	<10°
PSH250	61.5	6.01	1.72	20.2	89.4	1.17	0.25	0.27	0.37	nd	7.47	7.84	nd	69.1	119°
PSH300	63.8	6.17	1.85	18.2	90.0	1.16	0.21	0.24	0.32	nd	6.60	6.92	0.05	73.5	118°
PSH350	67.1	5.63	1.92	14.3	89.0	1.01	0.16	0.18	nd	nd	6.48	6.48	0.17	95.6	112°
PSH400	69.2	4.30	2.34	12.9	88.7	0.75	0.14	0.17	nd	0.30	5.13	5.43	0.02	80.3	92.4°
PSH450	67.6	3.21	2.47	17.4	90.7	0.57	0.19	0.22	nd	nd	6.11	6.11	nd	99.8	<10°
PSH500	67.9	2.84	2.32	17.8	90.8	0.50	0.20	0.23	nd	0.08	6.27	6.35	0.03	133	<10°

Table S4. Structural parameters derived from MultiCP/MAS ^{13}C NMR

Sample	0-62 ppm	62-92 ppm	92-150 ppm		150-165 ppm	165-190 ppm	190-220 ppm	[a]F_{aro}%	[b]F_{alkyl}%	[c]Polar carbon%	F_{Haro}/F_{aro}	[d]F_{aro}/F_{alkyl}	[e]$\chi_{edge,}$ min	[f]$\chi_{edge,}$ max	[g]n_c
	F_{nalk}%	F_{Oalk}%	F_{naro}%	F_{Haro}%	F_{Oaro}%	F_{COO}%	$F_{C=O}$%								
OS	56.1	3.12	17.7	15.0	4.45	3.03	0.62	37.1	59.2	11.2	0.40	0.63	0.52	2.14	2
Z300	41.9	2.42	25.3	25.4	4.02	0.82	0.38	54.5	44.3	7.64	0.46	1.23	0.54	1.35	4
Z400	12.1	3.03	55.8	25.2	2.61	0.63	0.68	83.6	15.1	6.95	0.30	5.54	0.33	0.51	23
Z500	2.13	1.70	74.8	17.8	2.14	0.97	0.37	94.8	3.83	5.18	0.19	24.7	0.21	0.25	96
ZHP300	40.4	3.34	29.4	20.0	4.85	1.75	0.33	54.2	43.7	10.3	0.37	1.24	0.46	1.27	4
ZHP400	12.0	3.75	54.8	27.3	1.38	0.67	0.00	83.5	15.8	5.80	0.33	5.29	0.34	0.54	21
ZHP500	3.04	2.55	72.2	17.7	2.55	1.46	0.00	92.4	5.59	6.56	0.19	16.5	0.22	0.28	76
ZSH300	40.3	4.44	38.0	8.73	4.99	2.96	0.56	51.7	44.8	13.0	0.17	1.16	0.27	1.14	5
ZSH400	11.7	3.86	53.9	21.4	4.83	2.60	1.71	80.2	15.5	13.0	0.27	5.16	0.33	0.54	21
ZSH500	2.90	2.26	71.8	17.7	2.79	2.52	0.05	92.3	5.16	7.62	0.19	17.9	0.22	0.28	76
PHP300	54.3	2.88	18.6	13.9	4.61	4.16	1.56	37.1	57.2	13.2	0.38	0.65	0.50	2.08	2
PHP400	33.5	2.43	31.0	28.4	3.01	1.59	0.11	62.4	35.9	7.14	0.45	1.74	0.50	1.08	6
PHP500	4.00	2.39	68.1	18.5	3.92	2.65	0.44	90.5	6.39	9.40	0.20	14.2	0.25	0.32	58
PSH300	57.1	3.82	20.4	9.57	4.06	3.94	1.10	34.8	60.9	12.9	0.28	0.56	0.40	2.22	2
PSH400	33.2	3.55	36.5	23.4	2.85	0.53	0.00	62.8	36.7	6.93	0.37	1.71	0.42	1.00	6
PSH500	6.44	3.93	63.2	22.2	2.43	1.00	0.78	87.9	10.4	8.14	0.25	8.47	0.28	0.41	36

[a]F_{aro}(92-165 ppm)=F_{Oaro} + F_{naro} + F_{Haro}; [b]F_{alkyl}(0-92 ppm)=F_{nalk}+ F_{Oalk};[c]Polar carbon%=F_{Oalk}%+F_{Oaro}%+F_{COO}%+$F_{C=O}$%;[d]F_{aro}/F_{alkyl}=$F_{aro}/(F_{Oalk}+F_{nalk})$;

[e]$\chi_{edge,\ min}=(F_{Haro}+F_{Oaro})/F_{aro}$;[f]$\chi_{edge,\ max}=\chi_{edge,\ min} + (F_{alkyl} + F_{C=O}) / F_{aro}$;[g]$n_C \geq 6/\chi^2_{edge} \geq 6/\chi^2_{edge,\ max}$ [14]

Table S5. Micropore volumes and mesopore volumes for Z-BCs before and after the solvent extraction

Sample	Dubinin-Radushkevitch		Cumulative micropore volume[a]			DFT	N_2 adsorption		
	CO_2-V_o	CO_2-*SSA*	0.37-0.7 nm	0.7-1.1 nm	>1.1 nm[b]	V_o[c]	V_t[e]	V_{micro}[f]	V_{meso}[g]
	μL/g	m^2/g	μL/g (%)[d]	μL/g (%)[d]	μL/g (%)[d]	μL/g	μL/g	μL/g	μL/g
Z250	43.5	108	13.1 (36.2)	4.50 (12.4)	11.8 (51.4)	36.2	0.21	0.02	0.07
Z300	41.3	103	14.5 (39.2)	4.70 (12.7)	13.7 (48.1)	37.0	--	--	--
Z350	68.5	171	23.9 (48.2)	6.70 (13.5)	17.7 (38.3)	49.6	0.25	0.03	0.10
Z400	132	329	43.7 (46.8)	15.7 (16.8)	32.8 (36.3)	93.3	68.2	49.0	19.2
Z450	210	523	46.0 (36.1)	17.2 (13.5)	64.4 (50.4)	127	349	289	60.0
Z500	256	638	45.5 (31.1)	17.8 (12.2)	82.5 (56.7)	146	464	384	80.0
After solvent extraction									
E-Z250	63.4	158	18.9 (52.9)	5.04 (14.1)	18.6 (33.0)	35.7	--	--	--
E-Z300	67.5	168	22.0 (51.6)	6.90 (16.2)	17.8 (32.2)	42.6	--	--	--
E-Z350	76.4	191	21.2 (44.3)	8.95 (18.7)	19.0 (37.0)	47.9	--	--	--
E-Z400	136	340	45.4 (48.2)	16.0 (17.0)	33.9 (34.8)	94.2	--	--	--
E-Z450	220	548	50.8 (37.0)	22.0 (16.0)	64.1 (46.9)	137	344	287	57.0
E-Z500	258	644	47.6 (32.0)	18.6 (12.5)	83.0 (55.5)	149	446	381	65.0

[a] Cumulative micropore volume is calculated by using density functional theory (DFT) of CO_2 adsorption.

[b] >1.1 nm is calculated from micropore areas at > 1.1 nm for DFT model of CO_2 adsorption. V=(4/3)*r*SSA, $r_{(CO2)}$=0.253 nm.[15]

[c] DFT-V_o is sum of micropore volumes at 0.37-0.7 nm, 0.7-1.1 nm, and >1.1 nm.

[d] (%) is the percentage of cumulative volume accounting for DFT-V_o.

[e] V_t is the total pore volumes at p/p_o=0.85 of N_2 adsorption.

[f] V_{micro} is the micropore volumes determined by DR model of N_2 adsorption.

[g] V_{meso} is the mesopore volumes determined by BJH model of N_2 adsorption.

Table S6. Micropore volumes and mesopore volumes on the activated and oxidized BCs.

Sample	Dubinin-Radushkevitch		[a]Cumulative micropore volumes			DFT	N_2 adsorption		
	CO_2-V_o	CO_2-*SSA*	0.37-1.1 nm	0.7-1.1 nm	>1.1 nm[b]	V_o[c]	V_t[e]	V_{micro}[f]	V_{meso}[g]
	μL/g	m^2/g	μL/g (%)[d]	μL/g (%)[d]	μL/g (%)[d]	μL/g	μL/g	μL/g	μL/g
OS	35.3	88.1	9.50 (40.2)	2.90 (12.3)	11.2 (47.5)	23.6	12.9	0.69	6.45
ZHP250	42.3	106	12.4 (43.8)	4.00 (14.1)	11.9 (42.1)	28.3	--	--	--
ZHP300	47.7	119	15.2 (46.2)	4.60 (14.0)	13.1 (39.8)	32.9	--	--	--
ZHP350	69.8	174	25.7 (51.1)	7.90 (15.7)	16.7 (33.2)	50.3	--	--	--
ZHP400	119	297	42.7 (50.1)	14.7 (17.2)	27.9 (32.7)	85.3	--	--	--
ZHP450	173	432	46.5 (41.1)	19.2 (17.0)	47.6 (42.0)	113	267	226	41.0
ZHP500	227	567	50.7 (36.1)	23.2 (16.5)	66.6 (47.4)	140	376	314	62.0
ZSH250	37.2	92.8	10.2 (42.0)	3.50 (14.4)	10.6 (43.5)	24.3	0.22	0.02	0.07
ZSH300	42.6	106	12.5 (43.8)	4.10 (14.4)	11.9 (41.8)	28.5	0.16	0.01	0.03
ZSH350	60.3	150	22.0 (50.9)	7.10 (16.4)	14.1 (32.6)	43.2	--	--	--
ZSH400	97.8	244	38.7(53.6)	12.0 (16.6)	21.5 (29.8)	72.2	--	--	--
ZSH450	177	438	53.9 (45.0)	19.6 (16.3)	46.4 (38.7)	120	222	188	34.0
ZSH500	221	552	51.1 (37.0)	23.6 (17.1)	63.5 (46.0)	138	350	294	56.0
PHP250	27.7	69.2	5.60 (33.7)	2.40 (14.5)	8.60 (51.8)	16.6	1.35	0.07	0.37
PHP300	26.4	66.0	5.20 (33.4)	1.90 (12.2)	8.47 (54.4)	15.6	1.98	0.11	0.60
PHP350	23.6	58.9	4.20 (31.1)	1.70 (12.6)	7.62 (56.4)	13.5	4.65	0.21	1.13
PHP400	36.6	91.2	8.70 (37.9)	3.40 (14.8)	10.9 (47.3)	23.0	5.12	0.35	1.88
PHP450	108	270	48.4 (58.3)	12.7 (15.3)	21.9 (26.4)	83.0	8.17	1.65	3.42
PHP500	131	328	66.3 (63.4)	16 .1 (15.4)	22.2 (21.2)	105	30.0	5.02	19.7
PSH250	25.9	64.7	5.00 (32.8)	2.10 (13.8)	8.13 (53.4)	15.2	2.15	0.10	0.66
PSH300	25.4	63.5	4.90 (32.9)	1.80 (12.1)	8.20 (55.0)	14.9	2.48	0.10	0.50
PSH350	24.8	61.9	4.00 (28.4)	1.90 (13.5)	8.16 (58.0)	14.1	3.31	0.14	0.72
PSH400	36.8	92.0	8.70 (36.7)	3.10 (13.1)	11.9 (50.2)	23.7	4.52	0.32	1.36
PSH450	97.0	243	46.0 (61.0)	11.0 (14.6)	18.4 (24.4)	75.4	3.37	0.48	1.14
PSH500	114	284	61.0 (66.1)	13.8 (15.0)	17.4 (18.9)	92.2	3.31	0.33	0.95

[a] Cumulative micropore volume is calculated by using density functional theory (DFT) of CO_2 adsorption.

[b] >1.1 nm is calculated from micropore areas at > 1.1 nm for DFT model of CO_2 adsorption. V=(4/3)*r*SSA, $r_{(CO2)}$=0.253 nm.[15]

[c] DFT-V_o is sum of micropore volumes at 0.37-0.7 nm, 0.7-1.1 nm, and >1.1 nm.

[d] (%) is the percentage of cumulative volume accounting for DFT-V_o.

[e] V_t is the total pore volumes at p/p_o=0.85 of N_2 adsorption.

[f] V_{micro} is the micropore volumes determined by DR model of N_2 adsorption.

[g] V_{meso} is the mesopore volumes determined by BJH model of N_2 adsorption.

Table S7. Sorption parameters of phenanthrene obtained by the *DR* model.

Sample	logQ_o' (μL /g)	CO_2-V_o μL/g	Q_o' μL/g [a](%)	*D*	R^2	*N*
OS	1.41	35.3	25.5 (72.2)	0.183	0.968	18
E-Z250	1.59	63.4	39.3 (62.0)	0.166	0.966	12
E-Z300	1.83	67.5	68.1 (101)	0.170	0.985	13
E-Z350	2.03	76.4	106 (139)	0.128	0.986	14
E-Z400	2.10	136	126 (92.6)	0.111	0.971	10
E-Z450	2.20	220	158 (71.8)	0.113	0.979	12
E-Z500	2.30	258	200 (77.5)	0.097	0.980	12
ZHP250	1.32	42.3	20.7 (48.9)	0.163	0.971	18
ZHP300	1.60	47.7	39.7 (83.2)	0.150	0.955	19
ZHP350	1.76	69.8	57.6 (82.5)	0.136	0.977	20
ZHP400	1.90	119	78.6 (66.1)	0.110	0.964	19
ZHP450	1.93	173	86.0 (49.7)	0.093	0.949	19
ZHP500	1.98	227	94.4 (41.6)	0.074	0.941	19
ZSH250	1.42	37.2	26.2 (70.4)	0.187	0.982	18
ZSH300	1.44	42.6	27.8 (65.3)	0.179	0.988	20
ZSH350	1.52	60.3	33.3 (55.2)	0.145	0.981	19
ZSH400	1.77	97.8	58.9 (60.2)	0.164	0.975	19
ZSH450	1.92	177	84.1 (47.5)	0.113	0.957	19
ZSH500	2.09	221	122 (55.2)	0.114	0.964	19
PHP250	1.30	27.7	19.8 (71.5)	0.228	0.984	17
PHP300	1.43	26.4	27.2 (103)	0.220	0.994	18
PHP350	1.56	23.6	36.1 (153)	0.230	0.993	17
PHP400	1.68	36.6	47.6 (130)	0.150	0.980	18
PHP450	1.60	108	39.7 (36.7)	0.146	0.982	17
PHP500	1.29	131	19.3 (14.7)	0.112	0.993	16
PSH250	1.14	25.9	13.7 (52.9)	0.179	0.950	16
PSH300	1.28	25.4	19.0 (74.8)	0.178	0.959	18
PSH350	1.53	24.8	33.6 (135)	0.170	0.973	20
PSH400	1.73	36.8	53.5 (145)	0.131	0.961	18
PSH450	1.36	97.0	22.9 (23.6)	0.128	0.943	19
PSH500	0.94	114	8.71 (7.64)	0.175	0.925	18

[a](%) is the percentage of adsorption volumes calculated by the *DR* model accounting for the micropore volumes.

Table S8. Freundlich parameters for the sorption and desorption, and hysteresis index of benzene on inactivated BCs*.

Sample	Sorption				Desorption				Hysteresis index (HI)[b]		
	$\log K_F$	n	R^2	N	$\log K_F$	n	R^2	N	p/p_o=0.003	p/p_o=0.03	p/p_o=0.3
R250	2.000 (0.035)[a]	0.588 (0.026)[a]	0.98	12	2.251 (0.014)	0.274 (0.011)	0.98	12	10.0	4.36	1.60
R300	2.068 (0.021)	0.460 (0.016)	0.99	12	2.295 (0.007)	0.239 (0.005)	0.99	12	5.09	2.66	1.20
R350	2.086 (0.031)	0.571 (0.023)	0.98	12	2.343 (0.011)	0.275 (0.008)	0.99	12	9.09	4.10	1.58
R400	2.097 (0.014)	0.389(0.010)	0.99	12	2.329 (0.003)	0.264 (0.002)	1.00	12	2.53	1.65	0.98
R450	2.112 (0.007)	0.389 (0.010)	1.00	12	2.211 (0.007)	0.204 (0.005)	0.99	12	1.18	0.75	0.41
R500	1.861 (0.010)	0.289 (0.007)	0.99	12	1.979 (0.024)	0.209 (0.018)	0.93	12	1.09	0.74	0.44

[a]Standard deviation

[b] $HI=\frac{V_g^d-V_g^s}{V_g^s}|_{T,P}$

* the data are cited from Zhang et al., (2014)[1].

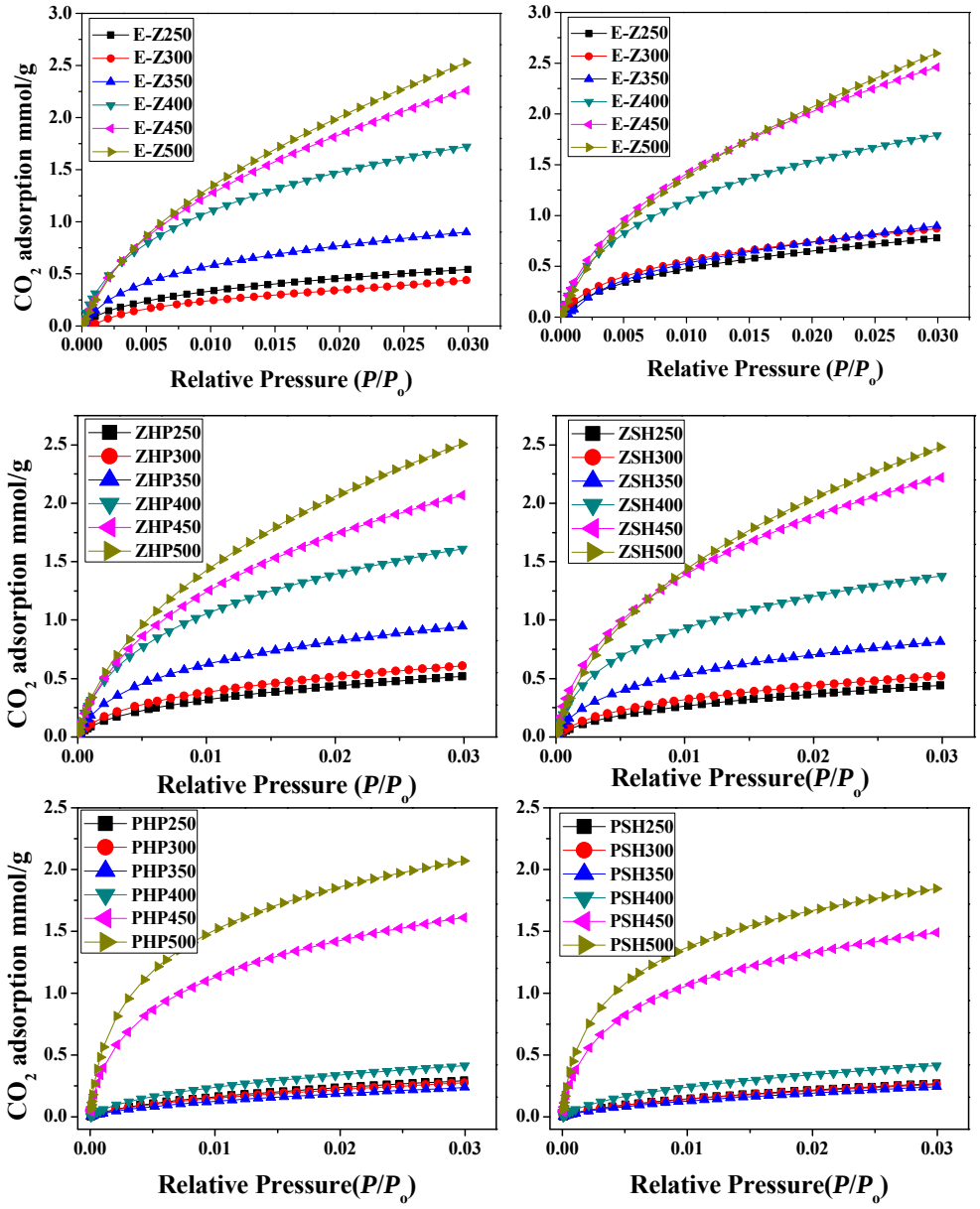

Figure S1. Carbon dioxide adsorption isotherms of BCs.

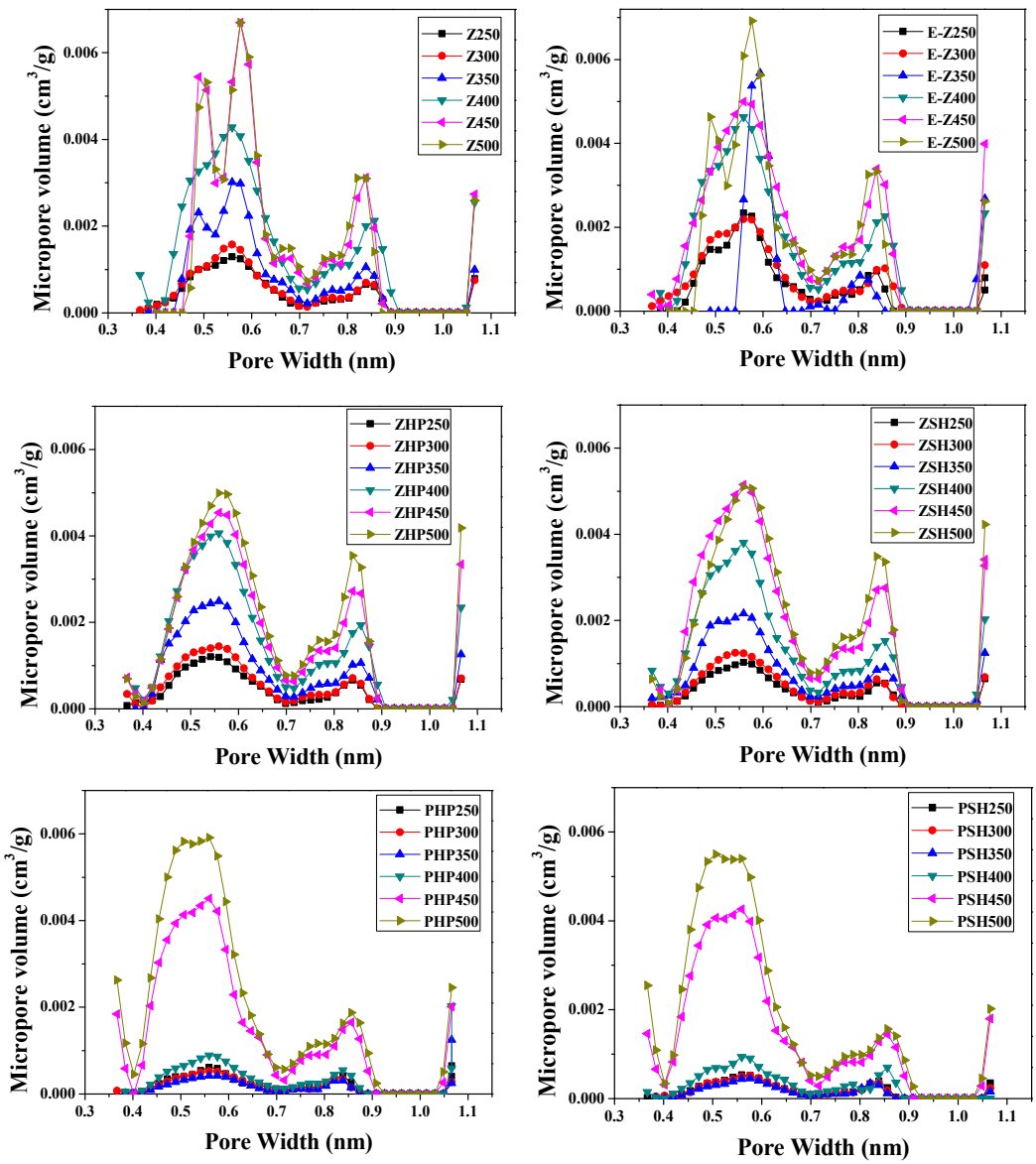

Figure S2. Micropore size distributions of BCs.

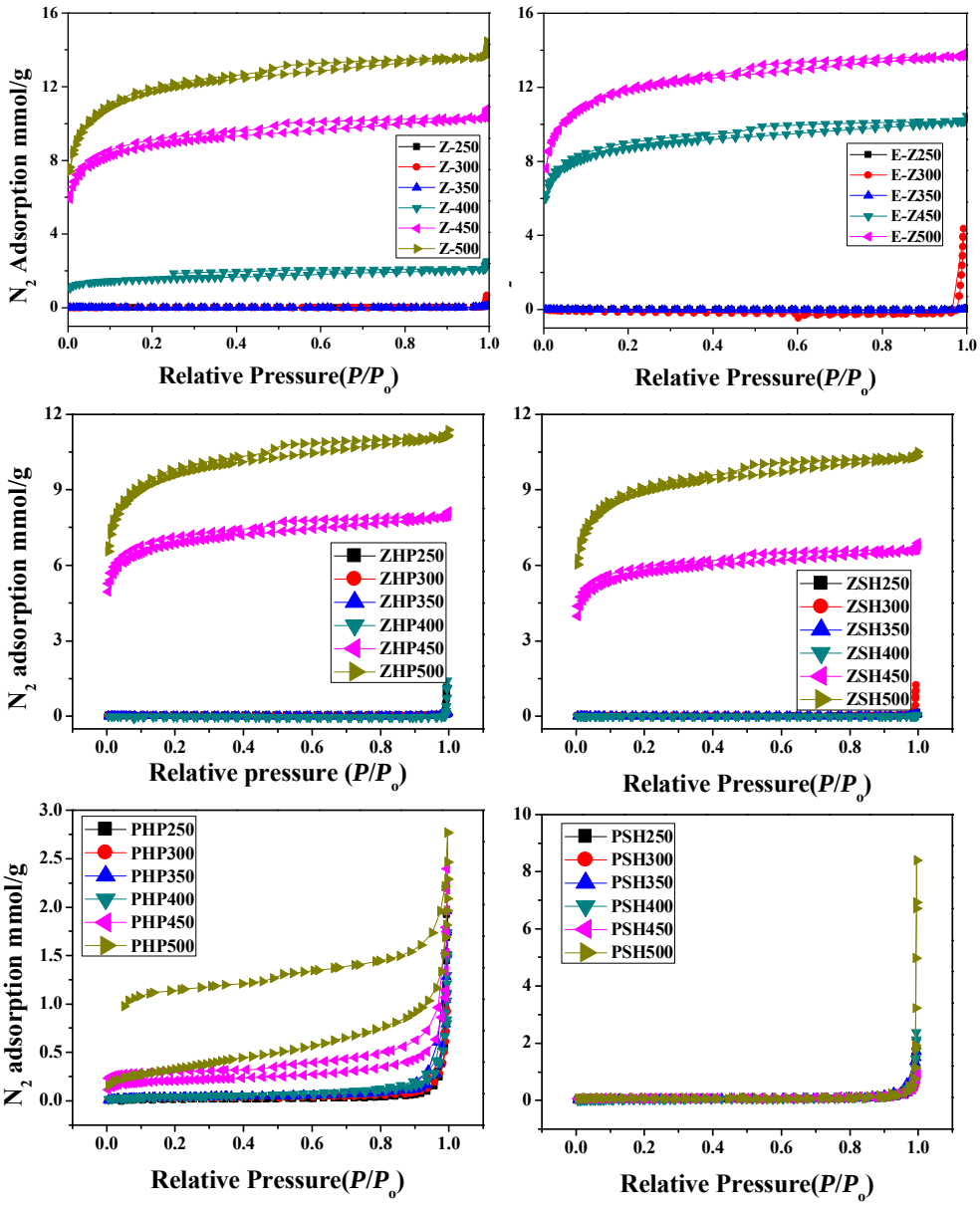

Figure S3. N_2 adsorption and desorption isotherms of BCs

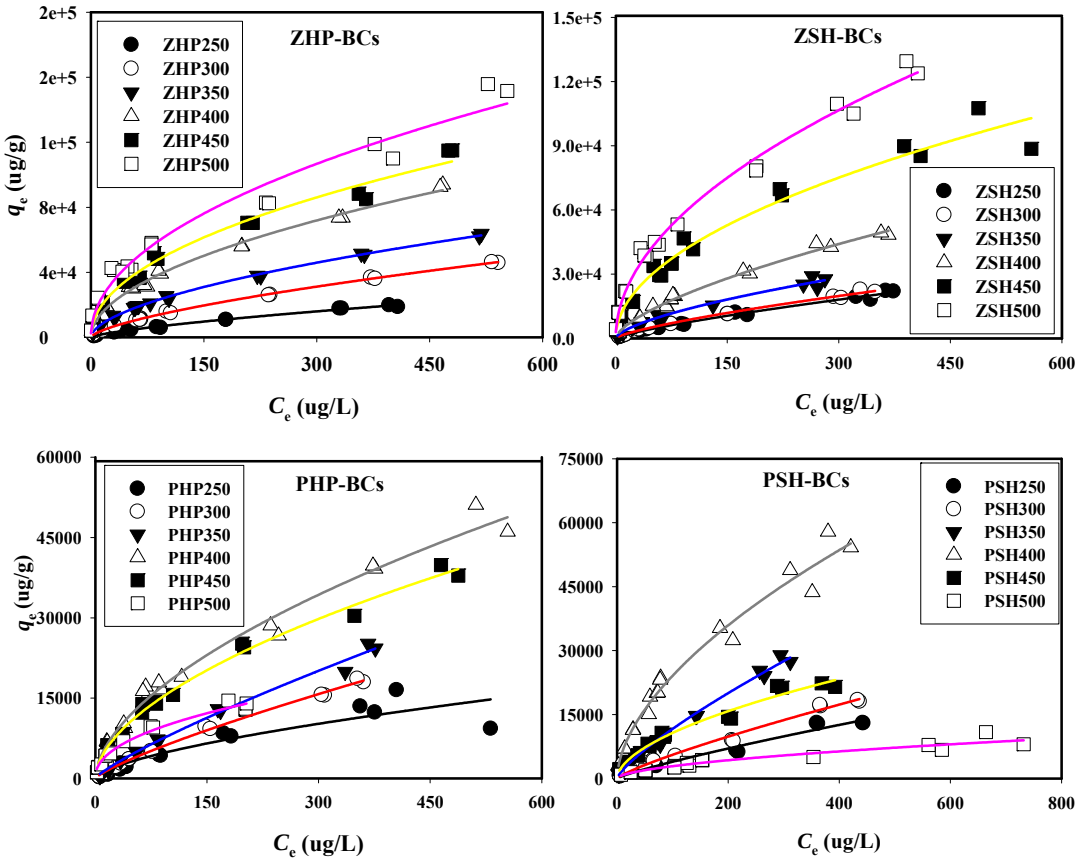

Figure S4. Sorption isotherms of phenanthrene on $ZnCl_2$- or KOH- activated and oxidized BCs.

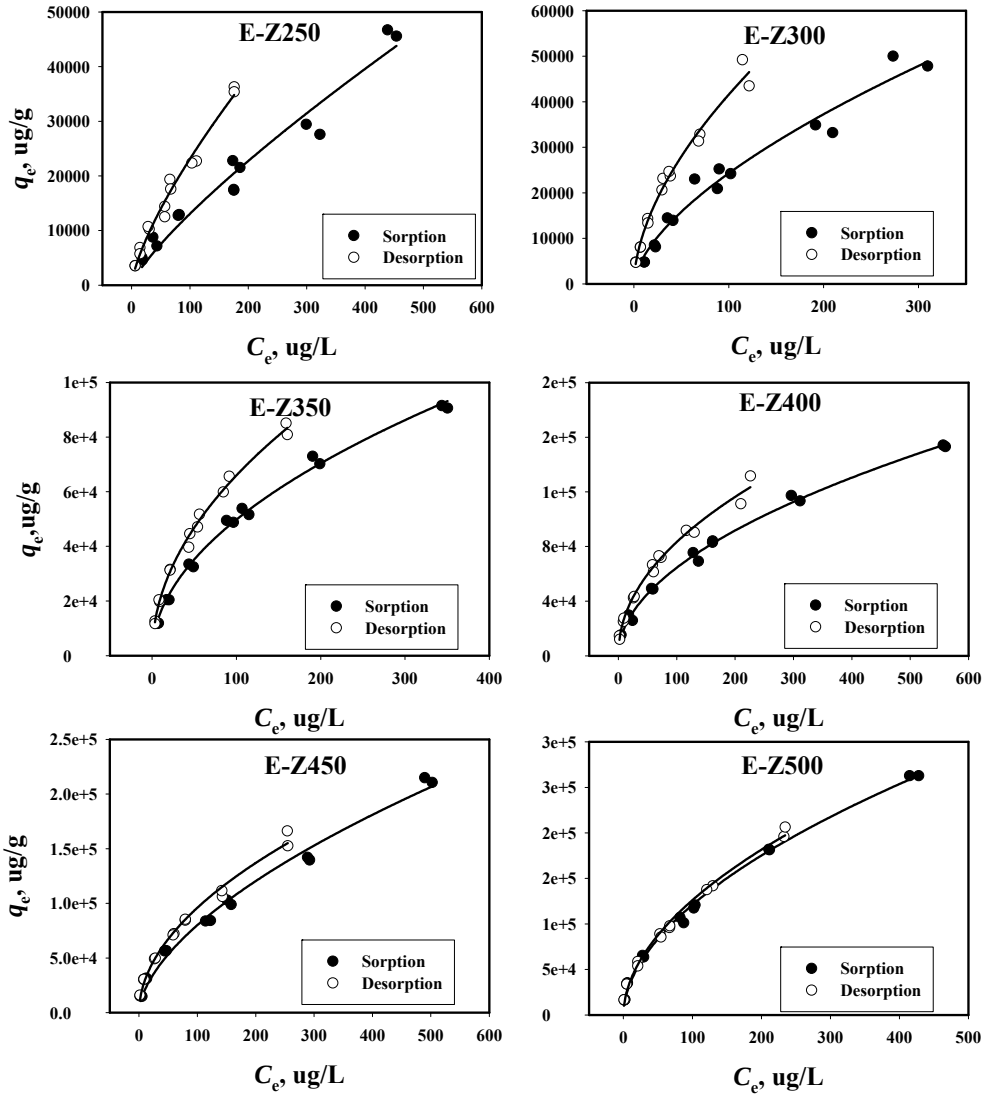

Figure S5. Sorption and desorption isotherms of phenanthrene on extracted $ZnCl_2$-activated BCs.

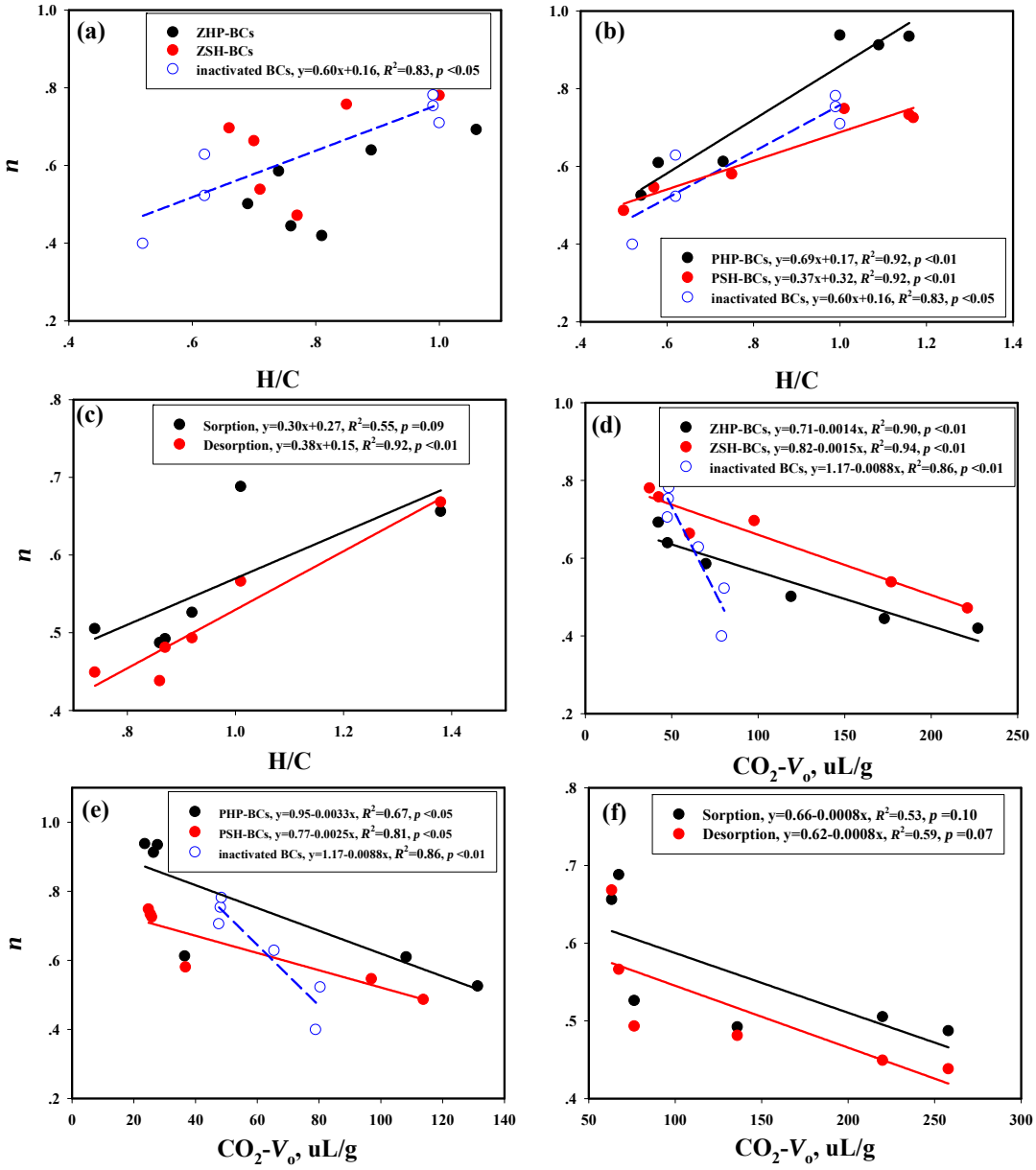

Figure S6. The relationships among the *n* values of phenanthrene with the values of H/C and CO_2-V_o on BCs.

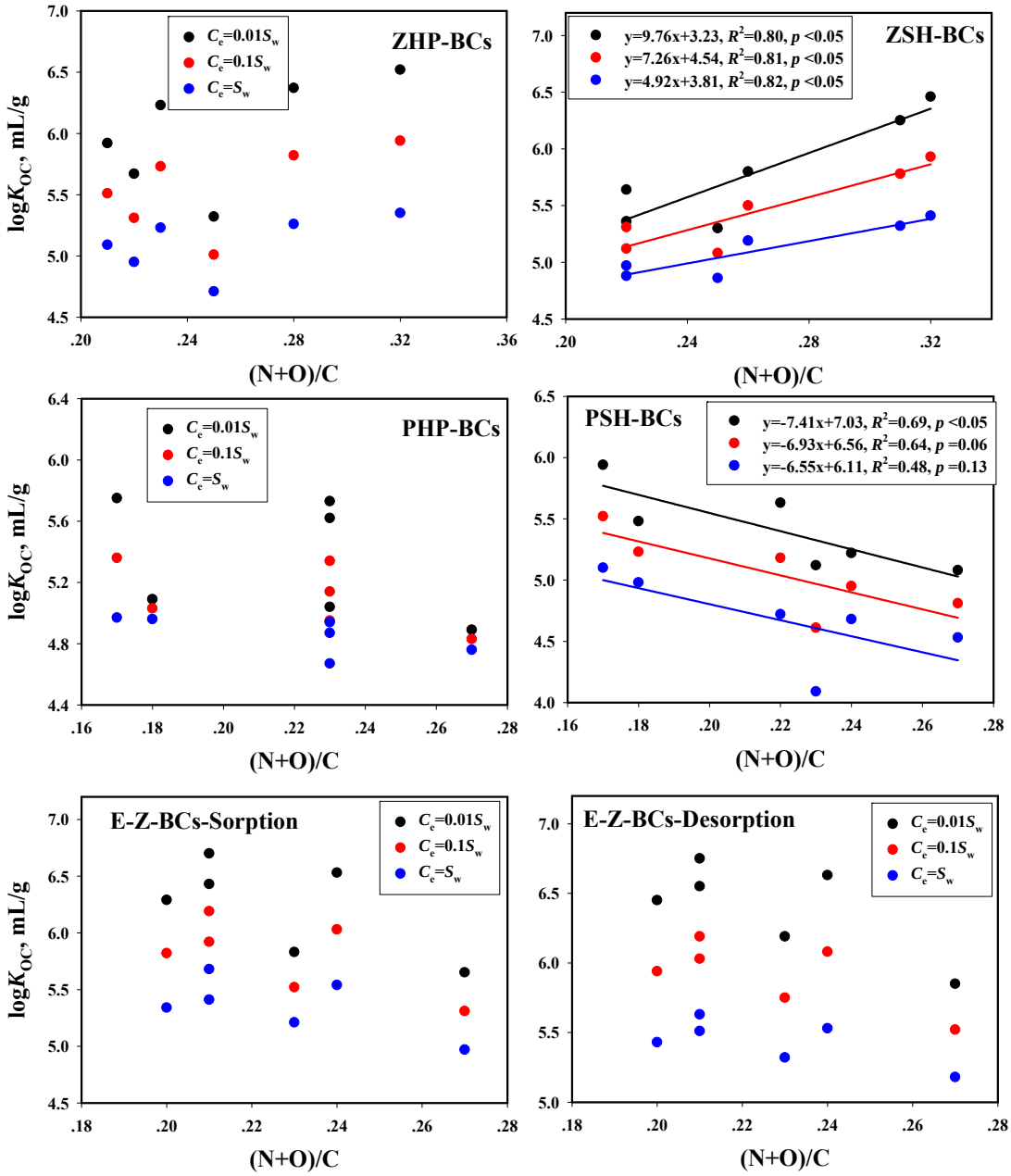

Figure S7. The relationships between the sorption capacity log K_{OC} of phenanthrene and the polarity factor (N+O)/C on BCs. In the graph, the black dots and lines represent C_e=0.01S_w, the red dots and lines C_e=0.1S_w, and the blue dots and lines C_e=S_w.

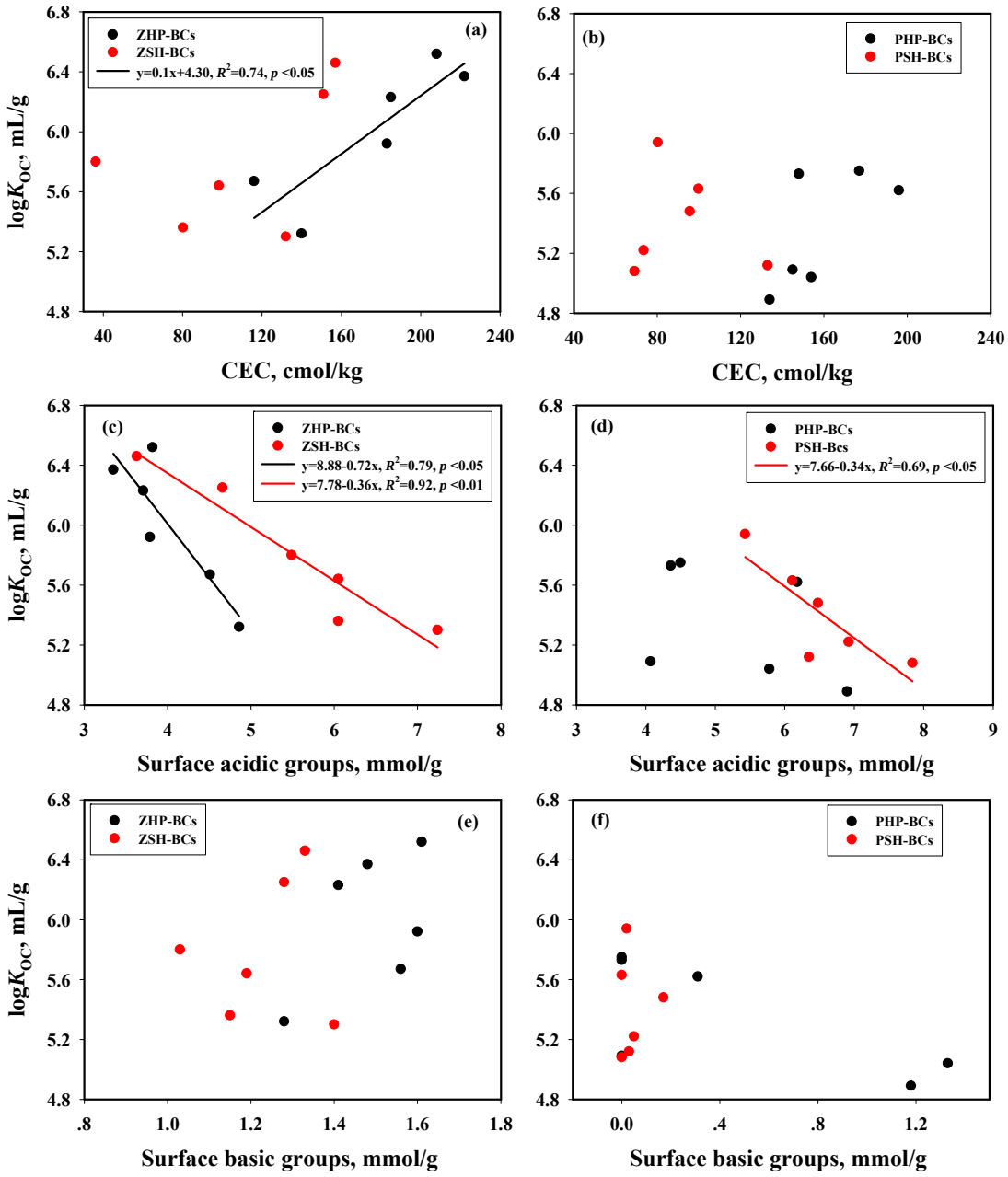

Figure S8. The relationships among the log K_{OC} (C_e=0.01S_w) values of phenanthrene with CEC values and surface amphoteric properties on $ZnCl_2$ or KOH activated and oxidized BCs.

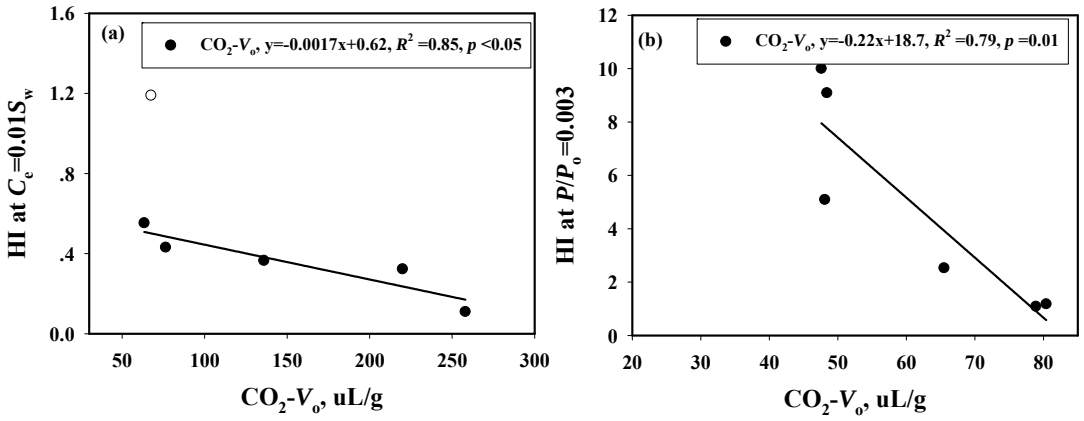

Figure S9. The relationships of the HI values with the values of CO_2-V_o on BCs. Graph (a) was the desorption of phenanthrene on E-Z-BCs and graph (b) was the desorption of benzene on inactivated kerogen BCs.

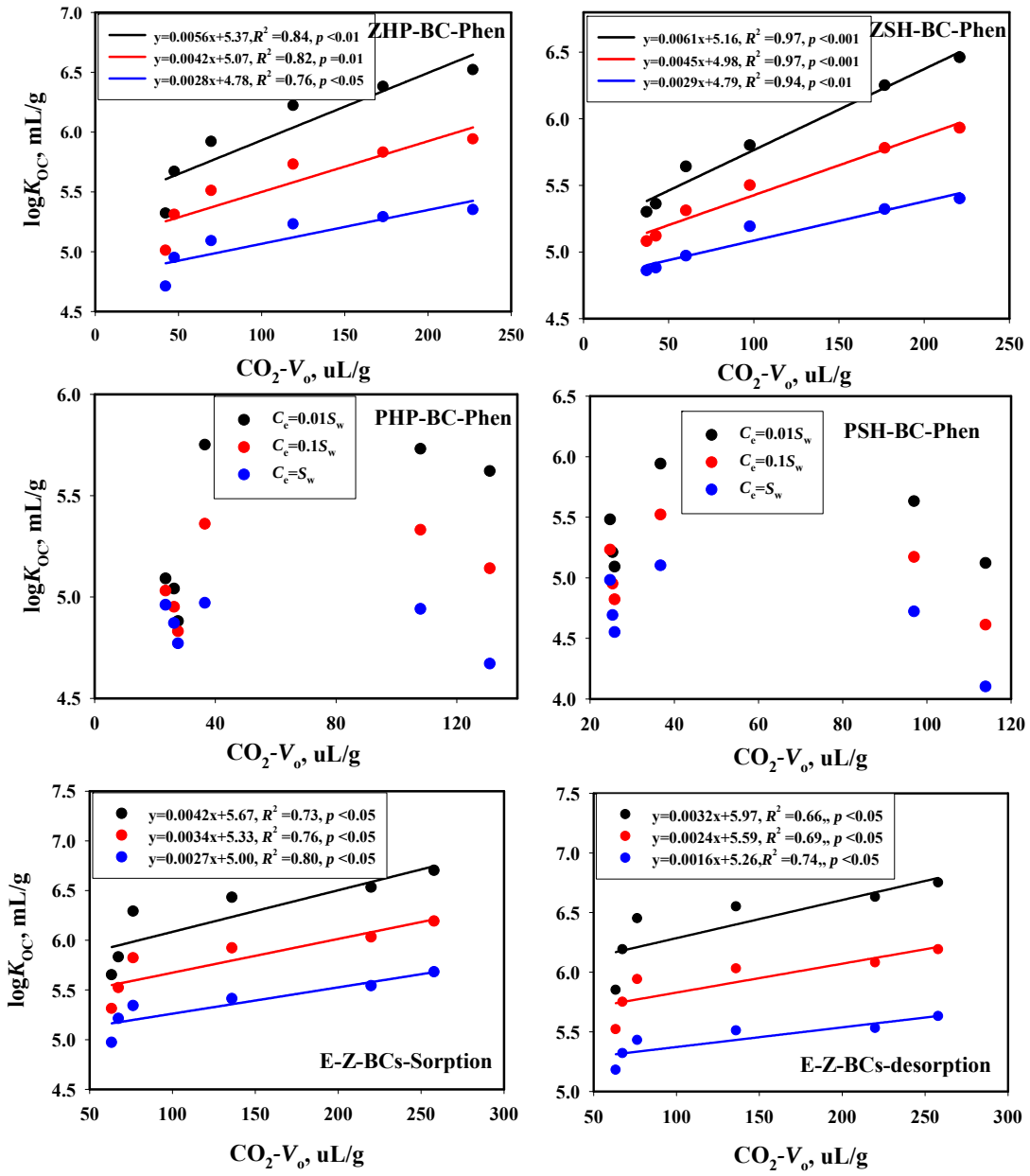

Figure S10. The relationships between the sorption capacity log K_{OC} of phenanthrene and the micropore volumes (CO_2-V_o) on BCs. In the graph, the black dots and lines represent C_e=0.01S_w, the red dots and lines C_e=0.1S_w, and the blue dots and lines C_e=S_w.

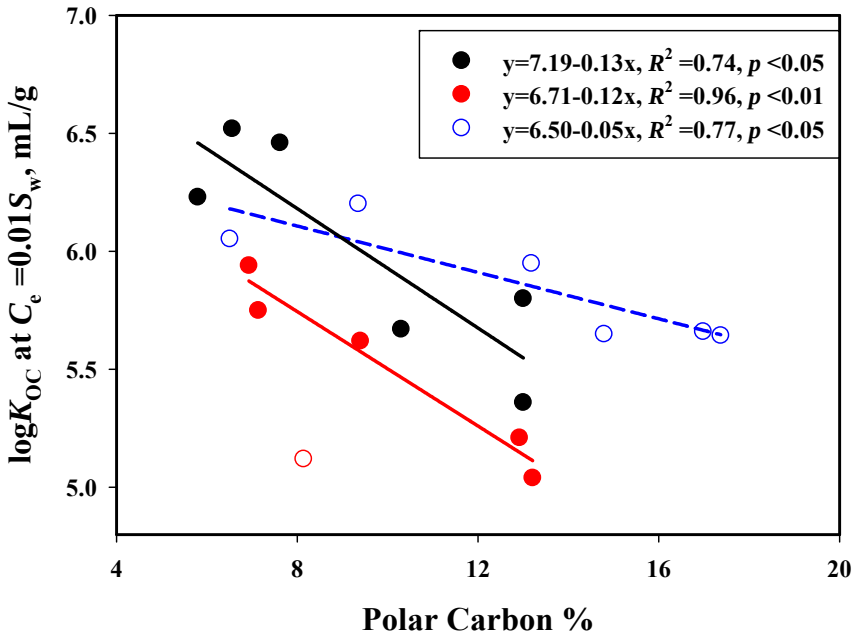

Figure S11. The relationships between the $\log K_{OC}$ (C_e=0.01S_w) values of phenanthrene with polar carbon on the $ZnCl_2$ or KOH activated and oxidized BCs. (In the graph, black lines are ZHP-BCs and ZSH-BCs, red lines are PHP-BCs and PSH-BCs, and blue lines are inactivated kerogen-derived samples. The outlier of PSH500 was shown in the red blank circle and not included in the corresponding correlation equation.)

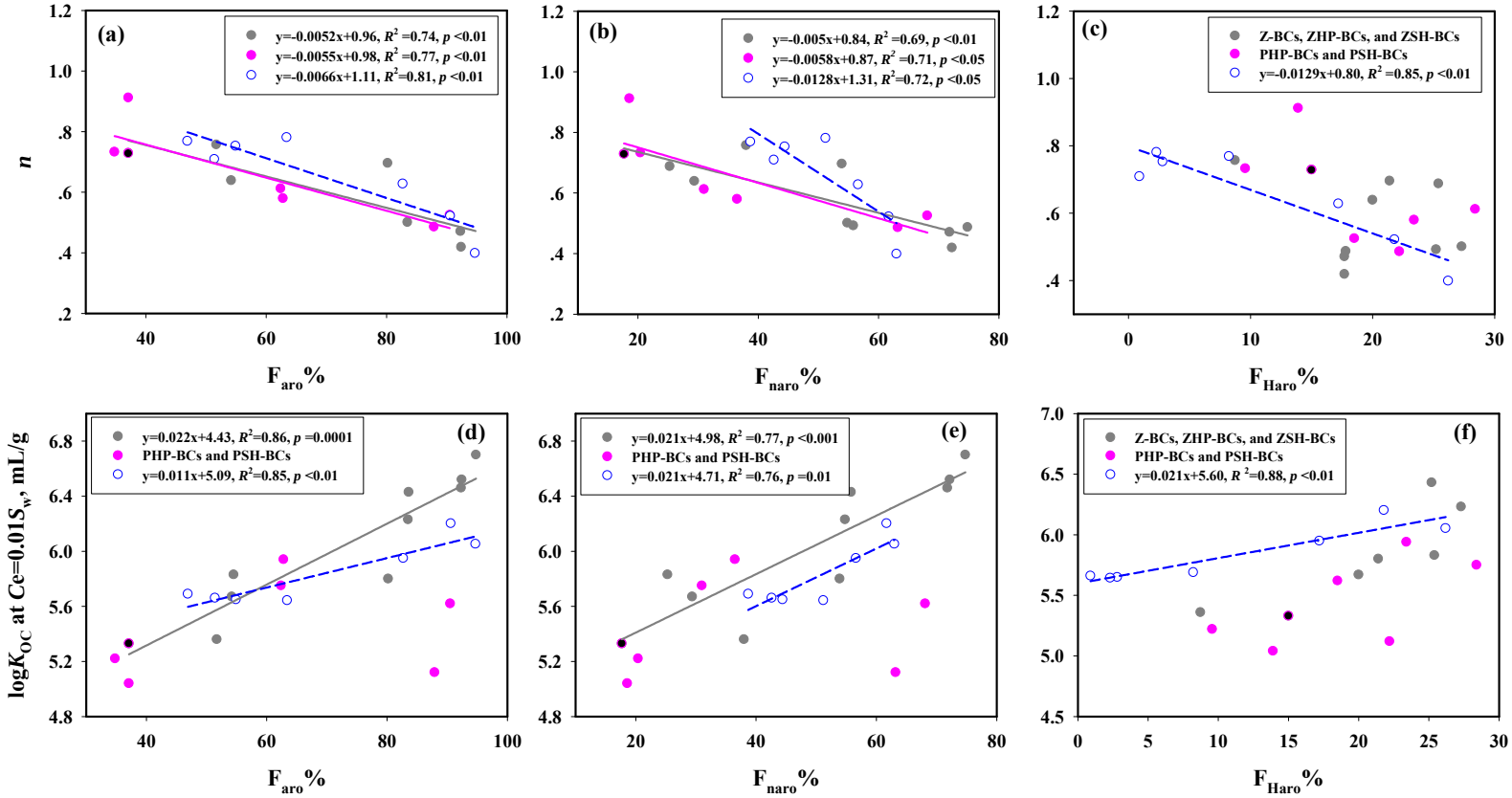

Figure S12. The relationships of the log K_{OC} and n of phenanthrene with F_{aro}%, F_{naro}%, and F_{Haro}% on the BCs. In the graph, the gray lines represent the ZHP-BCs and ZSH-BCs, the pink lines represent the PHP-BCs and PSH-BCs, and the blue lines represent the inactivated kerogen-derived BCs. The black dots represent OS and are included in the correlation equation.

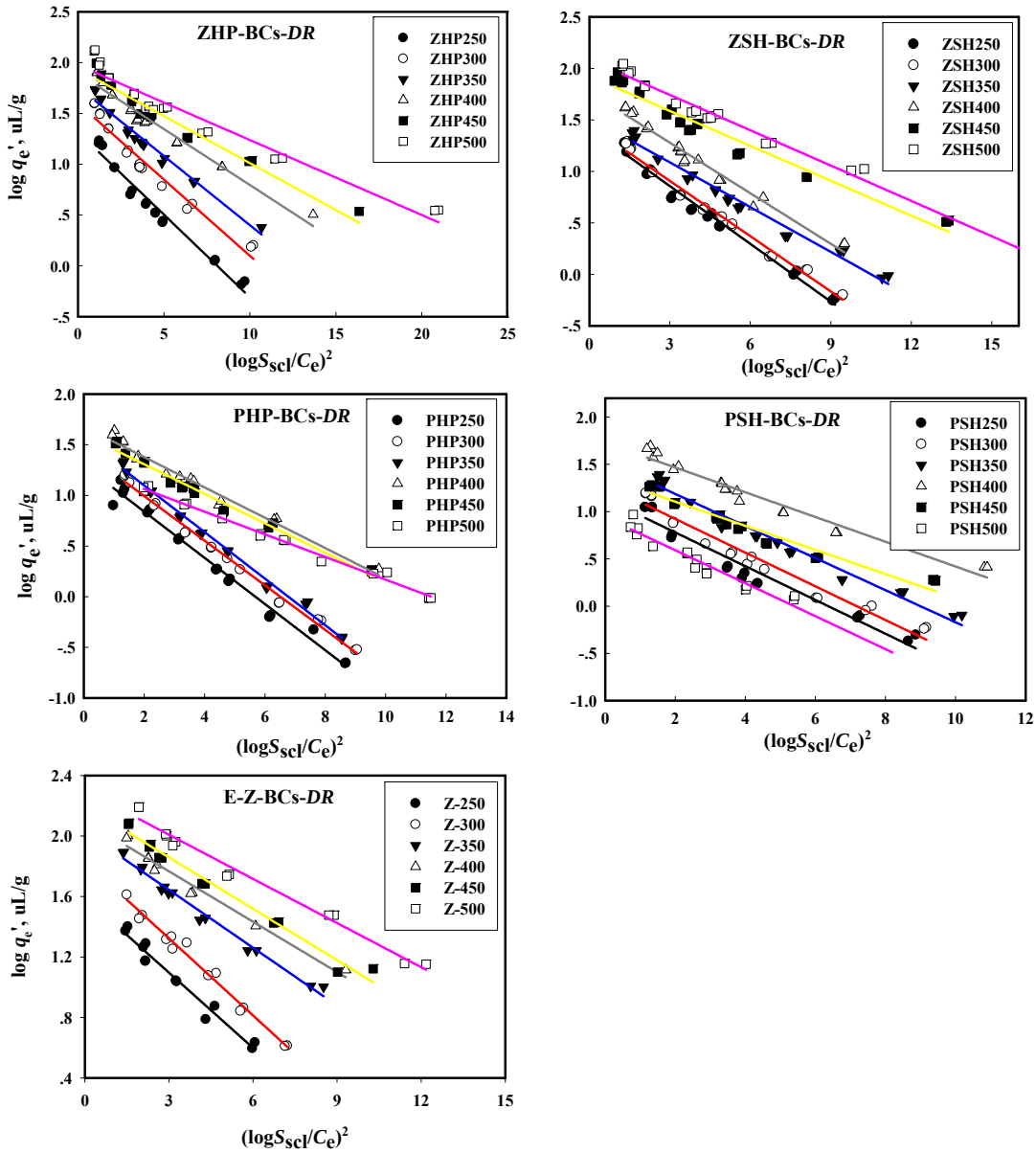

Figure S13. Sorption isotherms of phenanthrene on BCs described by the *DR* model.

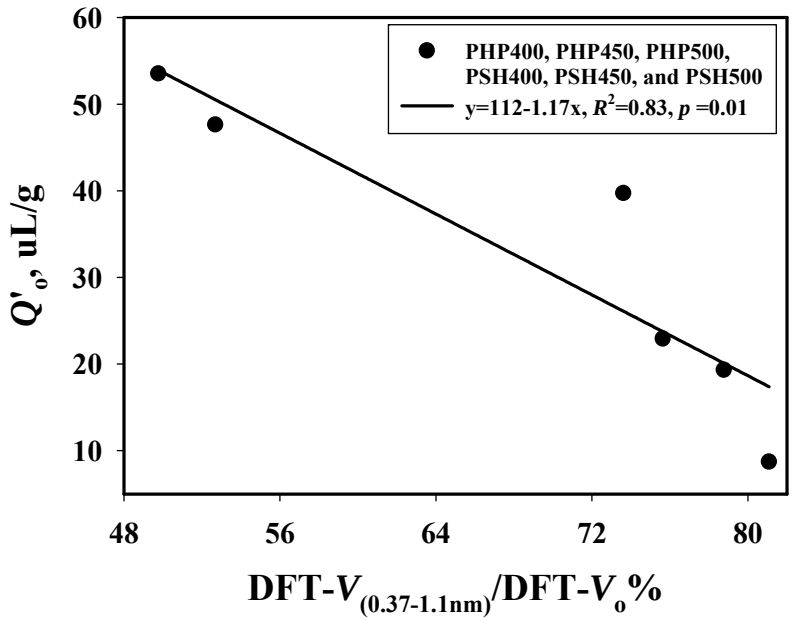

Figure S14. The relationships between the adsorption volumes Q_o' of phenanthrene and the DFT-$V_{(0.37\text{-}1.1nm)}$/DFT-V_o % on BCs.

Reference

(1) Zhang, Y.; Ma, X.; Ran, Y., Sorption of phenanthrene and benzene on differently structural kerogen: important role of micropore-filling. *Environ. Pollut.* **2014,** *185*, 213-218.

(2) Yang, J.; Qiu, K., Preparation of activated carbons from walnut shells via vacuum chemical activation and their application for methylene blue removal. *Chem. Eng. J.* **2010,** *165*, (1), 209-217.

(3) Yang, J.; Qiu, K. Q., Preparation of activated carbon by chemical activation under vacuum. *Environ. Sci. Technol.* **2009,** *43*, (9), 3385.

(4) Oliveira, L. C.; Pereira, E.; Guimaraes, I. R.; Vallone, A.; Pereira, M.; Mesquita, J. P.; Sapag, K., Preparation of activated carbons from coffee husks utilizing $FeCl_3$ and $ZnCl_2$ as activating agents. *J. Hazard. Mater.* **2009,** *165*, (1), 87-94.

(5) Ahmadpour, A.; Do, D., The preparation of activated carbon from macadamia nutshell by chemical activation. *Carbon* **1997,** *35*, (12), 1723-1732.

(6) Lillo-Ródenas, M. A.; Ros, A.; Fuente, E.; Montes-Morán, M. A.; Martin, M. J.; Linares-Solano, A., Further insights into the activation process of sewage sludge-based precursors by alkaline hydroxides. *Chem. Eng. J.* **2008,** *142*, (2), 168-174.

(7) Dıaz-Terán, J.; Nevskaia, D.; Fierro, J.; López-Peinado, A.; Jerez, A., Study of chemical activation process of a lignocellulosic material with KOH by XPS and XRD. *Micropor. Mesopor. Mater.* **2003,** *60*, (1), 173-181.

(8) Lozano-Castello, D.; Calo, J.; Cazorla-Amoros, D.; Linares-Solano, A., Carbon activation with KOH as explored by temperature programmed techniques, and the effects of hydrogen. *Carbon* **2007,** *45*, (13), 2529-2536.

(9) Zhang, D.; Duan, D.; Huang, Y.; Yu, Y.; Yong, R., Novel phenanthrene sorption mechanism by two pollens and their fractions. *Environ. Sci. Technol.* **2016,** *50*, (14), 7305-7314.

(10) Ran, Y.; Sun, K.; Yang, Y.; Xing, B.; Zeng, E., Strong sorption of phenanthrene by condensed organic matter in soils and sediments. *Environ. Sci. Technol.* **2007,** *41*, (11), 3952-3958.

(11) Kleineidam, S.; Schüth, C.; Grathwohl, P., Solubility-normalized combined adsorption-partitioning sorption isotherms for organic pollutants. *Environ. Sci. Technol.* **2002,** *36*, (21), 4689-4697.

(12) Ran, Y.; Xing, B.; Rao, P. S. C.; Fu, J., Importance of adsorption (hole-filling) mechanism for hydrophobic organic contaminants on an aquifer kerogen isolate. *Environ. Sci. Technol.* **2004,** *38*, (16), 4340-4348.

(13) Duan, D.; Zhang, D.; Ma, X.; Yang, Y.; Ran, Y.; Mao, J., Chemical and structural characterization of thermally simulated kerogen and its relationship with microporosity. *Mar. Petrol. Geol.* **2018,** *89*, 4-13.

(14) Mao, J.; Fang, X.; Lan, Y.; Schimmelmann, A.; Mastalerz, M.; Xu, L.; Schmidt-Rohr, K., Chemical and nanometer-scale structure of kerogen and its change during thermal maturation investigated by advanced solid-state ^{13}C NMR spectroscopy. *Geochim. Cosmochim. Acta* **2010,** *74*, (7), 2110-2127.

(15) Ran, Y.; Yang, Y.; Xing, B.; Pignatello, J. J.; Kwon, S.; Su, W.; Zhou, L., Evidence of micropore filling for sorption of nonpolar organic contaminants by condensed organic matter. *J. Environ. Qual.* **2013,** *42*, (3), 806-814.